

Amplifier-free slab-coupled optical waveguide optoelectronic oscillator systems

William Loh,^{1,2,*} Siva Yegnanarayanan,¹ Jonathan Klamkin,³ Shannon M. Duff,⁴ Jason J. Plant,¹ Frederick J. O'Donnell,¹ and Paul W. Juodawlkis¹

¹Lincoln Laboratory, Massachusetts Institute of Technology, 244 Wood Street, Lexington, Massachusetts 02420, USA

²Massachusetts Institute of Technology, 50 Vassar Street, Cambridge, Massachusetts 02139, USA

³Currently with Institute of Communication, Information and Perception Technologies, Scuola Superiore Sant'Anna, Pisa 56124, Italy

⁴Currently with National Institute of Standards and Technology, 325 Broadway, Boulder, Colorado 80305, USA

*William.Loh@ll.mit.edu

Abstract: We demonstrate a free-running 3-GHz slab-coupled optical waveguide (SCOW) optoelectronic oscillator (OEO) with low phase-noise (<-120 dBc/Hz at 1-kHz offset) and ultra-low sidemode spurs. These sidemodes are indistinguishable from noise on a spectrum analyzer measurement (>88 dB down from carrier). The SCOW-OEO uses high-power low-noise SCOW components in a single-loop cavity employing 1.5-km delay. The noise properties of our SCOW external-cavity laser (SCOWECL) and SCOW photodiode (SCOWPD) are characterized and shown to be suitable for generation of high spectral purity microwave tones. Through comparisons made with SCOW-OEO topologies employing amplification, we observe the sidemode levels to be degraded by any amplifiers (optical or RF) introduced within the OEO cavity.

©2012 Optical Society of America

OCIS codes: (140.0140) Lasers and laser optics; (250.0250) Optoelectronics.

References and links

1. X. S. Yao and L. Maleki, "Optoelectronic microwave oscillator," *J. Opt. Soc. Am. B* **13**(8), 1725–1735 (1996).
2. X. S. Yao and L. Maleki, "Optoelectronic oscillator for photonic systems," *IEEE J. Quantum Electron.* **32**(7), 1141–1149 (1996).
3. Y. K. Chembo, K. Volyanskiy, L. Larger, E. Rubiola, and P. Colet, "Determination of phase noise spectra in optoelectronic microwave oscillators: a Langevin approach," *IEEE J. Quantum Electron.* **45**(2), 178–186 (2009).
4. C. Henry, "Theory of spontaneous emission noise in open resonators and its application to lasers and optical amplifiers," *J. Lightwave Technol.* **4**(3), 288–297 (1986).
5. D. Eliyahu, D. Seidel, and L. Maleki, "RF amplitude and phase-noise reduction of an optical link and an optoelectronic oscillator," *IEEE Trans. Microw. Theory Tech.* **56**(2), 449–456 (2008).
6. D. Eliyahu, D. Seidel, and L. Maleki, "Phase noise of a high performance OEO and an ultra low noise floor cross-correlation microwave photonic homodyne system," in *Proc. FCS*, (2008), pp. 811–814.
7. C. W. Nelson, A. Hati, and D. A. Howe, "Relative intensity noise suppression for RF photonic links," *IEEE Photon. Technol. Lett.* **20**(18), 1542–1544 (2008).
8. P. S. Deygan, V. J. Urick, J. F. Diehl, and K. J. Williams, "Improvement in the phase noise of a 10 GHz optoelectronic oscillator using all-photonic gain," *J. Lightwave Technol.* **27**(15), 3189–3193 (2009).
9. W. Zhou, O. Okusaga, C. Nelson, D. Howe, and G. Carter, "10 GHz dual loop opto-electronic oscillator without RF-amplifiers," in *Proc. SPIE*, (2008), pp. 68970Z–1–68970Z–6.
10. W. Loh, F. J. O'Donnell, J. J. Plant, M. A. Brattain, L. J. Missaggia, and P. W. Juodawlkis, "Packaged, high-power, narrow-linewidth slab-coupled optical waveguide external cavity laser (SCOWECL)," *IEEE Photon. Technol. Lett.* **23**(14), 974–976 (2011).
11. J. Klamkin, S. M. Madison, D. C. Oakley, A. Napoleone, F. J. O'Donnell, M. Sheehan, L. J. Missaggia, J. M. Caissie, J. J. Plant, and P. W. Juodawlkis, "Uni-traveling-carrier variable confinement waveguide photodiodes," *Opt. Express* **19**(11), 10199–10205 (2011).
12. P. W. Juodawlkis, J. J. Plant, W. Loh, L. J. Missaggia, F. J. O'Donnell, D. C. Oakley, A. Napoleone, J. Klamkin, J. T. Gopinath, D. J. Ripin, S. Gee, P. J. Delfyett, and J. P. Donnelly, "High-power, low-noise 1.5- μ m slab-coupled optical waveguide (SCOW) emitters: physics, devices, and applications," *IEEE J. Sel. Top. Quantum Electron.* **17**(6), 1698–1714 (2011).
13. X. S. Yao and L. Maleki, "Ultralow phase noise dual-loop optoelectronic oscillator," in *Proc. OFC*, (1998), pp. 353–354.

14. W. Zhou and G. Blasche, "Injection-locked dual opto-electronic oscillator with ultra-low phase noise and ultra-low spurious level," *IEEE Trans. Microw. Theory Tech.* **53**(3), 929–933 (2005).
 15. O. Okusaga, E. J. Adles, E. C. Levy, W. Zhou, G. M. Carter, C. R. Menyuk, and M. Horowitz, "Spurious mode reduction in dual injection-locked optoelectronic oscillators," *Opt. Express* **19**(7), 5839–5854 (2011).
 16. W. Loh, J. Klamkin, S. M. Madison, F. J. O'Donnell, J. J. Plant, S. Yegnanarayanan, R. J. Ram, and P. W. Juodawlkis, "Slab-coupled optical waveguide (SCOW) based optoelectronic oscillator (OEO)," in *Proc. IPC*, (2011), pp. 605–606.
 17. C. H. Cox, *Analog Optical Links: Theory and Practice* (Cambridge University Press, 2004).
 18. G. E. Obarski and J. D. Splett, "Transfer standard for the spectral density of relative intensity noise of optical fiber sources near 1550 nm," *J. Opt. Soc. Am. B* **18**(6), 750–761 (2001).
 19. W. Loh, S. Yegnanarayanan, R. J. Ram, and P. W. Juodawlkis, "Super-homogeneous saturation of microwave-photonic gain in optoelectronic oscillator systems," *IEEE Photon. J.* **4**(5), 1256–1266 (2012).
 20. A. David and M. Horowitz, "Low-frequency transmitted intensity noise induced by stimulated Brillouin scattering in optical fibers," *Opt. Express* **19**(12), 11792–11803 (2011).
 21. K. S. Giboney, M. J. W. Rodwell, and J. E. Bowers, "Traveling-wave photodetector theory," *IEEE Trans. Microw. Theory Tech.* **45**(8), 1310–1319 (1997).
-

1. Introduction

The optoelectronic oscillator (OEO) is a system that uses optical downconversion to generate a stable microwave signal with low phase-noise [1, 2]. Potentially any RF frequency can be synthesized as long as the components of the optical cavity (e.g., modulator, photodetector) have the bandwidth required for operation. Unlike conventional electronic oscillators, the phase-noise of an OEO does not theoretically degrade at higher frequencies. Equivalently, the OEO quality factor (Q) increases with oscillation frequency, since the loss of optical fiber is constant for practically any RF frequency that can be generated. If oscillation can be achieved, the OEO phase-noise [1, 3] is dependent on thermal noise, shot noise, laser relative intensity noise (RIN), and optical fiber nonlinearities.

The phase-noise of an OEO can be made small because the delay-line used in the optical path can be made long with almost negligible increases in roundtrip loss. The delay-line acts as a filter for OEO noise similar to how an external cavity filters the noise of a semiconductor laser [4]. This filtering depends on the square of the delay-length, thus allowing the OEO phase-noise (free-running) to rival the best microwave oscillators [5–7]. However, due to nonlinearities in the transport of optical signals over fiber, the scaling laws of delay length usually break down at higher optical powers and longer delay lengths. These nonlinearities will be addressed in a later section. In addition to these issues, a long fiber delay causes the mode spacing to decrease below limits where the sidemodes can be filtered out by an RF filter. For 1 km of delay, the sidemode spacing is 200 kHz, which is below the bandwidths of typical filters at microwave frequencies.

Previous reports have shown that the OEO is capable of phase-noise as low as -160 dBc/Hz at 10-kHz offset oscillating at 10-GHz center frequency [5, 6]. This level of performance comes at the cost of noise due to the many sidemodes (>100 for a 16-km fiber delay) that compete for gain within the bandwidth of the RF filter. Typically, RF amplification is employed in an OEO to provide the gain necessary to oscillate. However, this is not always true as some OEOs have demonstrated oscillation using only the microwave-photonic (MWP) gain provided by a modulated optical source. In these cases, optical amplification was always still required and incorporated either internally to the OEO cavity [8] or externally to the laser source [7, 9]. The use of an optical amplifier is undesirable as it increases both the noise and power consumption of the OEO. In this work, we demonstrate a 3-GHz high-performance amplifier-free slab-coupled optical waveguide optoelectronic oscillator (SCOW-OEO). The OEO uses high-power low-noise slab-coupled optical waveguide (SCOW) laser sources and photodiodes to enable oscillation via MWP gain only [10–12]. No optical or RF amplifiers are used within the configuration of our system. We find that the SCOW-OEO demonstrates excellent phase-noise performance, even with only 1.5 km of delay length, due to the use of high-power, low-noise SCOW components. Comparisons to SCOW-OEO topologies that use RF amplification will also be made when possible. We show that the sidemodes of our amplifier-free system are at the level of noise on a spectrum analyzer measurement (>88 dB down from the carrier). These low sidemode spurs are

achieved without the use of dual-loop [13] or injection-locked [14, 15] configurations, which would otherwise increase the complexity or degrade the performance of our oscillator. Furthermore, we observe that the use of amplification (optical or RF) within the OEO cavity appears to significantly increase the level of the measured sidemodes.

2. SCOW-OEO system, operation, and components

A schematic of the SCOW-OEO system [16] is shown in Fig. 1. The system consists of a high-power low-noise slab-coupled optical waveguide external cavity laser (SCOWECL) ($P = 300$ mW at 4 A) [10, 12] and a high-power variable-confinement slab-coupled optical waveguide photodiode (VC-SCOWPD) ($BW = 3.5$ GHz, $I_{sat} = 38$ mA, $\mathcal{R} = 1$ A/W) [11]. The SCOWECL is modulated by a Mach-Zehnder (MZ) modulator ($BW = 15$ GHz, $V_{\pi} = 3.1$ V at 3 GHz, loss = 2.2 dB), and the resulting signal is sent to the VC-SCOWPD after passing

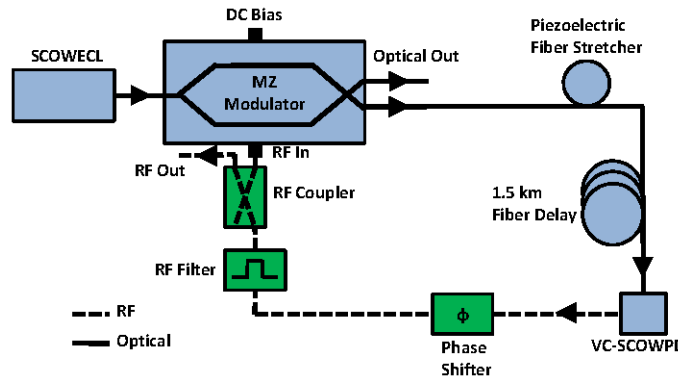


Fig. 1. Schematic of SCOW-OEO system.

through a fiber stretcher and 1.5 km fiber delay-line. The photodiode downconverts the optical signal into an RF photocurrent at the beat frequency of the optical modulation. This signal is sent to an RF phase shifter and an RF filter ($f_{center} = 3$ GHz, $BW = 2.5$ MHz) before being coupled out of a -10 dB RF coupler. The majority of the RF power is reused to drive the RF input port of the modulator to obtain self oscillation. The SCOWECL, modulator, fiber delay, and photodiode form an intensity modulated direct-detection (IMDD) link allowing signal amplification from modulator RF_{in} to photodiode RF_{out} . The piezoelectric fiber stretcher serves as a phase modulator for suppression of fiber nonlinearities (stimulated Brillouin scattering (SBS) and double backscattered interferometric noise) [5, 7]. The fiber stretcher was operated at resonance by driving it with a 60-kHz sinusoid having a peak-to-peak voltage of 30 V. The RF filter defines the center frequency of oscillation and filters unwanted sidemodes/noise, while the RF phase shifter allows for static fine-tuning around this operating point. It is important to note that the SCOW-OEO does not employ any optical or RF amplification and thus oscillates solely from MWP gain [17].

OEO oscillation begins from noise entering the RF input port of the modulator. This noise can be generated by thermal noise, shot noise, and laser RIN or by noise from nonlinear optical fiber scattering. The incident noise causes a tiny modulation of the optical carrier, which is recovered as an RF signal after the photodetection process. If the RF signal (after one roundtrip) exceeds the original noise input into the modulator, the OEO achieves net gain and can therefore oscillate. The signal continues to become amplified with each roundtrip until saturation occurs. Usually, the saturation mechanism results from the modulator exceeding its linear range of operation but can also occur from compression of other components (e.g., photodiode, RF amplifier when present). For the SCOW-OEO, the dominant amplitude-limiting mechanism occurs through saturation of the modulator response. In steady-state, the gain saturates to approximately the level of the net intracavity loss. For more details regarding the operation of an OEO, we refer the reader to Ref [1].

Commonly, the phase-noise spectrum of high-performance OEOs degrades significantly from amplitude-to-phase (AM-PM) noise conversion during the photodetection process [5]. The photodiode must be biased at the null in the AM-PM conversion slope in order to suppress these effects. Lower performing OEOs are often limited by RF amplifier flicker noise instead. While the AM-PM process is important, the authors wish to make clear that even without any AM-PM conversion, intensity-noise still becomes the ultimate limit to OEO phase-noise. This is true because the injection of incoherent intensity noise on top of a coherent modulation signal perturbs the phase of the oscillation and results in broadening of the phase-noise spectrum. For this reason, it is essential for a high-performance OEO that all intensity-noise processes are reduced as much as possible. In the next two sections, we describe measurements of the RIN and AM-PM conversion noise for the SCOWECL and VC-SCOWPD used in the SCOW-OEO system.

2.1 SCOWECL relative intensity noise (RIN)

The RIN spectrum of the SCOWECL was determined by direct photodetection of the SCOWECL continuous wave (CW) optical power and subsequent measurement of the electrical noise signal on an Agilent 89410A vector signal analyzer. Figure 2(a) shows the measured low-frequency RIN of the SCOWECL and of a commercial high-performance external cavity laser (ECL). Both measurements were taken using the same experimental setup and calibrated using the RIN transfer standard method [18]. The RIN was measured in three separate intervals 10 Hz – 2 kHz (resolution bandwidth (RBW) = 10 Hz), 10 Hz – 100 kHz (RBW = 1 kHz), and 10 Hz – 2 MHz (RBW = 10 kHz). Points at frequencies close to the RBW of each measurement were discarded due to corruption from near-DC noise. In Fig. 2(a), we have also provided the RIN of a Lightwave Electronics Nd:YAG laser (obtained from Ref [5].) for comparison. Note that the relaxation resonance peak of the Nd:YAG laser is not shown here but can be found in Fig. 4 of Ref [5]. The SCOWECL RIN is 10-15 dB below

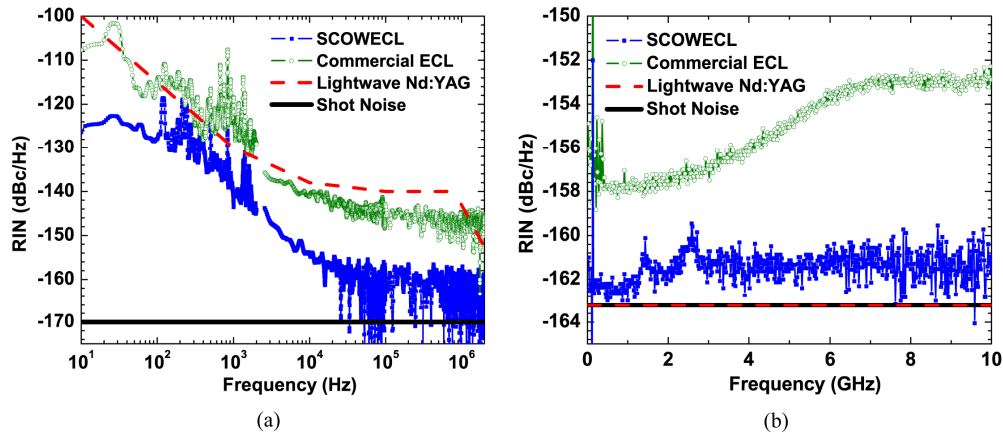


Fig. 2. Measured SCOWECL (solid squares) and commercial ECL (open circles) (a) low-frequency (10 Hz–2 MHz) and (b) high-frequency (10 Hz – 10 GHz) RIN with corresponding shot-noise floor (solid line). The RIN of a Lightwave Electronics Nd:YAG laser (dashed line) is also provided for comparison (assumed shot-noise limited at high-frequencies).

both the commercial ECL RIN and the Nd:YAG laser RIN throughout the measurement range (0-2 MHz) and also compares favorably against other semiconductor, fiber, and solid state lasers. We believe most of the peaks at low frequencies (100 Hz – 1 kHz) to be due to 60 Hz harmonics and technical noise.

Although we have thus far only discussed the low-frequency RIN of the SCOWECL, we wish to emphasize that the RIN at both low and high frequencies are important to an OEO. Oscillation starts through RIN at the oscillation frequency, and eventually causes the generation of sidebands through optical modulation of the carrier. The sideband generation

process results in the upconversion of low frequency RIN into the frequency band of the oscillation signal. The RIN around the carrier therefore becomes a weighted average of the RIN at low and high frequencies. Typically, low-frequency RIN dominates over high-frequency RIN, and the OEO's phase-noise spectrum follows the spectrum of the laser's low-frequency RIN. Figure 2(b) shows the measured high-frequency RIN for the SCOWECL and the commercial ECL from 10 Hz to 10 GHz. The expected RIN of the Lightwave Electronics Nd:YAG laser (shot-noise limited) is also provided for comparison. Again, the SCOWECL high-frequency RIN is lower than the commercial ECL RIN, but only by 4-8 dB for noise below 10 GHz. The commercial ECL exhibits a relaxation resonance peak between 6 and 10 GHz that increases its RIN to -153 dBc/Hz. For many semiconductor lasers, this resonance peak is even larger and can significantly increase the average RIN of the OEO. As can be seen in Fig. 2(b), the SCOWECL RIN spectrum is nearly shot-noise limited throughout the measurement range and thus exhibits similar high-frequency RIN to that of the Nd:YAG laser. Note that the shot-noise level is higher in Fig. 2(b) compared to Fig. 2(a) since a photodiode having higher bandwidth and lower saturation current was used for the high-frequency measurements. The SCOWECL also does not exhibit the relaxation resonance signature characteristic of typical lasers. The resonance is damped by the long photon lifetime due to the exceptionally low intracavity optical loss.

2.2 VC-SCOWPD AM and PM noise

In this section, we describe our measurements of the VC-SCOWPD's noise contribution to the SCOW-OEO phase-noise. As mentioned earlier, the photodetection process results in AM-PM noise conversion that broadens the phase-noise spectrum of the RF signal. The measured VC-SCOWPD amplitude response (open circles) and phase response (solid squares) are shown in Fig. 3 for DC photocurrents between 1 and 46 mA. These results were obtained through S21 measurements of the photodiode using an Agilent N5230C lightwave component analyzer

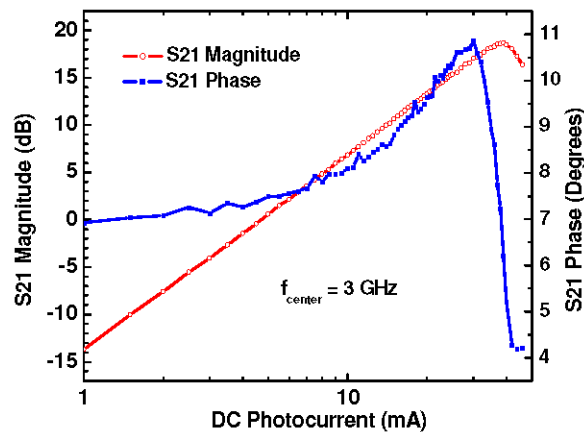


Fig. 3. Measured dependence of VC-SCOWPD phase (solid squares) and amplitude (open circles) on DC photocurrent at 3 GHz operation and -3.5 V DC bias.

(LCA). The measurement applies a 5 dBm RF modulation tone to an internal modulator and outputs a modulated optical signal for probing the VC-SCOWPD. The optical signal is externally amplified by a high-power erbium-doped fiber amplifier (EDFA) and subsequently attenuated using a variable optical attenuator for control of the optical power incident on the photodiode.

The DC photocurrent is a parameter that sets the operating point of the OEO since it is inherently related to the average optical power of an IMDD link. Intensity noise on top of the optical signal causes a fluctuation in this operating point, which leads to a fluctuation in the output RF signal. Both the amplitude and phase of the RF output are affected, but in nonlinear

ways due to the complicated behavior of carrier transport in the photodiode at higher photocurrent levels. Ideally, the phase response should be flat for OEO operation so that an intensity noise fluctuation causes nearly zero change in the RF output response. As can be observed in Fig. 3, the flat regions of phase response are located at low photocurrents (1-4 mA) and at a small window between 26 and 29 mA. It is essential for the SCOW-OEO to be operated at these points for the lowest phase-noise performance. In a similar vein, it is also beneficial for the amplitude response of the VC-SCOWPD to be operated at a region of zero slope. This allows for intensity fluctuations to become attenuated during the downconversion to RF, thus resulting in decreased OEO amplitude-noise. The zero-slope region of the amplitude response occurs near 38 mA for the measured VC-SCOWPD. It is ideal if both regions of zero-slope are collocated at a single photocurrent operation point. However, our measured VC-SCOWPD does not exhibit these characteristics for the applied reverse bias of -3.5 V.

3. Results and discussion

In this section, we detail our measurements assessing the performance of the 3-GHz SCOW-OEO whose configuration is shown in Fig. 1. We first describe measurements of the oscillator's phase-noise, which were obtained using a commercial Agilent E5052B signal-source analyzer (SSA). The measurement was performed by direct-detection of the signal out of the -10 dB OEO output port. The results of the high-performance RF-amplifier-free SCOW-OEO system are shown in Fig. 4(a) along with the noise-floor of the SSA system. The phase-noise is instrument noise-floor limited throughout almost the entire measurement range. Only at low frequencies (<100 Hz) does the OEO phase-noise rise above the measurement-limit of the SSA. Our measured sidemodes (at harmonics of 135 kHz corresponding to 1.5 km

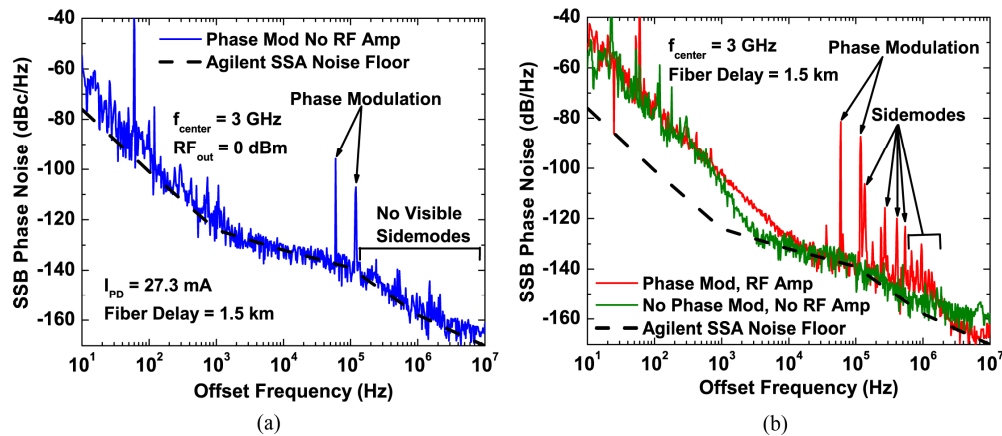


Fig. 4. Measured SCOW-OEO phase noise operating under (a) highest performance conditions (phase modulation, no RF amplification) and (b) lower performance conditions (phase modulation, RF amplification and no phase modulation, no RF amplification). The noise-floor of the SSA (dashed line) is also provided.

optical delay) are <-140 dBc/Hz. We thus achieve large sidemode suppression in our SCOW-OEO, even when multiple modes can oscillate within the bandwidth of the RF filter (2.5 MHz). This is due to the saturation properties of MWP gain resulting in the sidemodes experiencing less gain than the main oscillation mode of the cavity [19]. We experimentally optimized the SCOW-OEO's operating photocurrent around 27.3 mA. This agrees well with the minimum AM-PM conversion point for our photodiode as observed in Fig. 3. Finally, the RF output power taken from the -10 dB output coupler was measured to be 0 dBm. This corresponds to an intracavity RF power of ~ 10 dBm.

In Fig. 4(a), there are two visible spurs located at 60 kHz and 120 kHz that result from the applied phase modulation internal to the OEO cavity. This phase modulation is necessary in order to suppress the effects of fiber nonlinearities and interferometric noise. One common nonlinear noise source in optical fiber is SBS. Even below the SBS threshold, the associated intensity fluctuations can still dominate the low-frequency noise of an optical link [20]. The suppression of SBS through phase modulation is well-known and significantly reduces phase-noise in high-performance OEOs [5, 7]. With phase modulation, the spectrum is spread across the modulation harmonics and therefore suppresses SBS through the depletion of intensity in each field component. Interferometric noise resulting from double-backscattered optical signals also degrades the system noise at low frequencies. Reflections of the signal can theoretically occur at any interface of the optical cavity. We find these reflections to be most significant at the facet of the photodiode. In addition to phase modulation, optical isolation at the photodiode interface may be used to greatly suppress the influence of interferometric noise.

Figure 4(b) shows the measured phase-noise of the SCOW-OEO (i) without phase modulation and without RF amplification and (ii) with phase modulation and with RF amplification. The RF amplifier exhibits 28-dB gain with 4-dB noise figure and is located internal to the OEO RF cavity (after photodetection). Without phase modulation, the phase-noise degrades significantly (~ 20 dB) compared to that measured in Fig. 4(a) at low offset frequencies. The degradation of phase-noise at higher frequencies (>3 kHz) cannot be evaluated due to the limitation of the noise-floor. As expected, both the phase modulation spurs and sidemodes are absent in the phase-noise measurement. For the SCOW-OEO employing RF amplification, we find a similar degradation in its low-frequency phase-noise (~ 20 dB). The measurement of phase-noise at higher offset frequencies is again limited by the SSA noise-floor. Aside from introducing the amplifier, no other modifications were made to the system. With the amplifier in the system, we operated the VC-SCOWPD at 16 mA, instead of 27.3 mA. Although this is at a point with higher AM-PM conversion, we have verified that the OEO (with RF amplification) achieves similar performance across many different current ranges. This suggests that the RF amplifier's noise dominates over all other noise sources in the system. In Fig. 4(b), the phase modulation spurs are clearly visible at harmonics of 60 kHz. However, we find that after employing RF amplification, the sidemodes (at harmonics of 135 kHz) also appear in the measured phase-noise spectrum. The first sidemode spur reaches a level of -106 dBc/Hz, while the later spurs decrease gradually to the level of noise.

In Fig. 5, we show the measured RF spectrum of the SCOW-OEO under a variety of operating conditions. Figure 5(a) shows the normalized RF spectrum at offset frequencies close to the carrier (-2.5 kHz to 2.5 kHz). All four combinations with/without phase modulation and RF amplification were tested in our measurements. The resolution bandwidth was 100 Hz for this offset frequency range. The measured RF spectra agree with our findings of SCOW-OEO phase-noise in Fig. 4. The noise level is at its maximum when the SCOW-OEO is operated without phase modulation and with RF amplification. Furthermore, the noise levels are similar between the case employing phase modulation and RF amplification and the case using neither phase modulation nor RF amplification. Finally, the noise level of the SCOW-OEO is lowest when only phase modulation is used. Near zero offset frequency, the resolution bandwidth integrates over the oscillating signal and prevents the ability to resolve differences in noise.

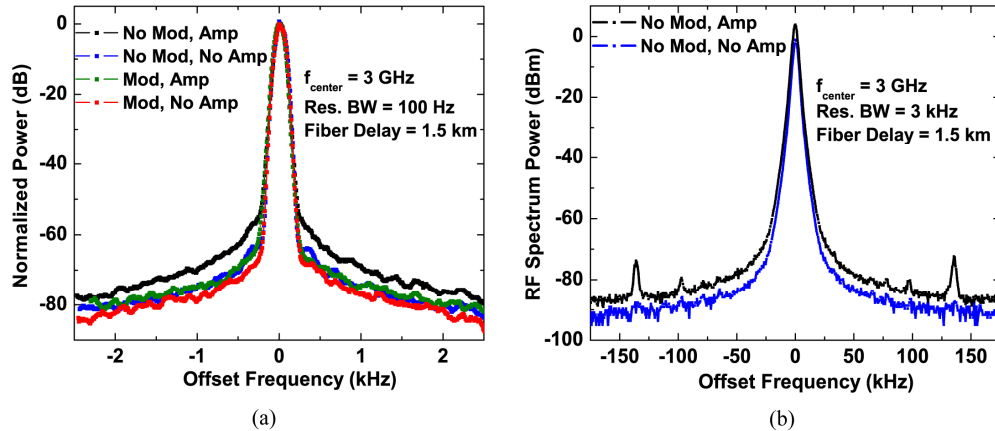


Fig. 5. Measured SCOW-OEO RF spectrum at (a) low offset frequencies (-2.5 kHz to 2.5 kHz) and (b) and high offset frequencies (-175 kHz to 175 kHz) under varying operating conditions.

Figure 5(b) shows the RF spectrum of the SCOW-OEO (without normalization) for larger offset frequencies between -175 kHz to 175 kHz using a resolution bandwidth of 3 kHz. For this experiment, the SCOW-OEO was operated with and without RF amplification. Phase modulation was not employed during either measurement. The RF power (including cable losses) out of the -10 dB RF coupler was found to be 3.8 dBm and -1.2 dBm with and without RF amplification, respectively. In Fig. 5(b), we subtracted out the spectrum analyzer noise floor so that the sidemodes could be made more apparent. The sidemodes are clearly visible at ± 135 kHz offset when an RF amplifier is used in the system. The measured sidemode level of -72.3 dBm results in a sidemode suppression of ~ 76 dB. For the amplifier-free SCOW-OEO system, the sidemodes cannot be seen above the level of noise. In this case, the sidemode suppression is measured to be >88 dB.

As our SCOW-OEO can operate without RF amplification, it is useful to discuss its performance characteristics for potential scaling to longer delays and higher frequencies. The SCOW-OEO exhibits a threshold of 20 mA, and we operate our system at 27.3 mA photocurrent. The net small signal power gain is 1.2 dB after accounting for MWP amplification and RF cavity loss. The combined loss for the components of the RF cavity (excluding the photodiode) is 2.8 dB. The bandwidth of the VC-SCOWPD (3.5 GHz) imposes an extra 2.1 dB of loss for operation at 3 GHz. This suggests the MWP link power gain to be 6.1 dB total. The net gain of the MWP link is 4.0 dB operating at 3 GHz after accounting for losses due to finite photodiode bandwidth. One can potentially increase the fiber delay from 1.5 km to 15 km for 20 dB improvement in SCOW-OEO phase-noise. However, the loss incurred through the additional delay is ~ 3.0 dB at 1550 nm (attenuation = 0.2 dB/km), and thus a doubling of the photocurrent (~ 27 mA to ~ 54 mA) is required to drive oscillation. The required photocurrent is within reach of the VC-SCOWPD technology. However, suppression of nonlinear fiber noise would be necessary for the benefits of delay to be fully realized. Currently the bandwidth of the VC-SCOWPD limits operation of the SCOW-OEO to a few GHz. Higher bandwidth VC-SCOWPDs (10 - 12 GHz) have been demonstrated with slightly reduced responsivity (0.7 A/W) and lower current handling capabilities (~ 30 mA) [11]. Traveling-wave electrode structures are required to extend the VC-SCOWPD technology beyond these operation regimes [21].

From Figs. 4 and 5, we found that the insertion of an RF amplifier significantly degraded the phase-noise performance of the SCOW-OEO. In our next experiment, we replace this generic component with a high-performance AMLPNC1002 RF amplifier designed for the purpose of low phase-noise. The amplifier exhibits 10.9 dB gain and 5.9 dB noise figure. The phase-noise at 100 Hz offset is specified to be -158.9 dBc/Hz. In addition to inserting the RF

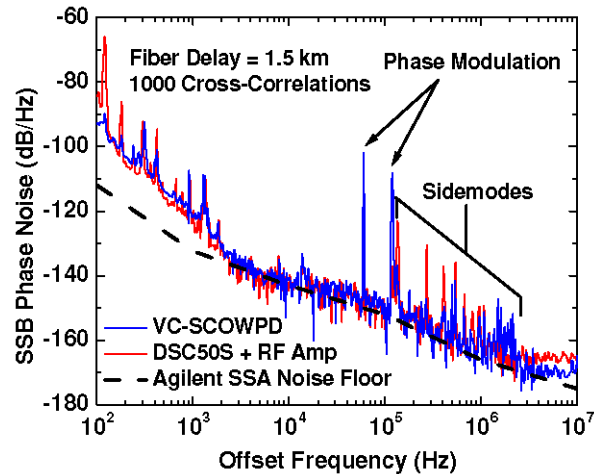


Fig. 6. Measured 3 GHz SCOW-OEO phase-noise for two configurations: one comprising a DSC50S + low-noise RF amplifier and one comprising a VC-SCOWPD. Cross-correlation averaging (1000x) was used for reducing the noise-floor (dashed line) of the measurement system.

amplifier, we also replace the VC-SCOWPD with a lower-power Discovery DSC50S photodiode. The purpose is to compare a commercial high-performance low-power detection link against the VC-SCOWPD for operation in the SCOW-OEO. Aside from these components, no other changes were made to the OEO system.

Figure 6 shows the phase-noise of the SCOW-OEO operated with the DSC50S + low-noise RF amplifier and also with the VC-SCOWPD. The system with the VC-SCOWPD is identical to that used in Fig. 4(a). Cross-correlation averaging (1000 times) was used in order to improve the SSA noise-floor. For Fig. 4, we decided not to use cross-correlation averaging due to the increase in required measurement time. Even with a reduced span, this increases the measurement time to nearly 7 minutes. The number of cross-correlations that can be practically applied is limited by the drift of our intensity modulator. The measured RF powers are -1.2 dBm and -5 dBm (including cable loss) for the VC-SCOWPD and DSC50S + low-noise RF amplifier systems, respectively. Phase modulation was employed for both measurements in order to suppress noise contributions from fiber nonlinearities. The measured phase-noise is comparable for both systems in the range of 100 Hz to 2 kHz. Above 2 kHz, both systems reach the SSA measurement-limit. Note that both measurements are noise-floor limited even in the range 3 MHz – 10 MHz (RF filter bandwidth ~ 2.5 MHz). The observed difference at high offset-frequency (3-10 MHz) results from the sensitivity of the SSA's minimum noise-floor to RF input power. The measured phase-noise performance is similar for both OEOs since the laser used is the same and because the RF amplifier noise [which degraded operation in Fig. 4(b)] is no longer a limitation. The sidemodes, however, are clearly larger for the system using RF amplification, as was also found to be the case in Fig. 4(b). The RF amplifier also adds additional size/weight and considerably raises total power consumption (>3 W). Averaging over drift and noise spikes during the 7-minute measurement causes the phase-noise to increase slightly above the values found in Fig. 4(a). It should be mentioned that the SCOW-OEO employing the VC-SCOWPD was operated at 27.3 mA photocurrent, which was the same as that used in Fig. 4(a). For the DSC50S + low-noise RF amplifier SCOW-OEO, we experimentally optimized its performance around 7 mA of photocurrent. This operating point agrees well with measurements of the minimum for the photodiode's AM-PM response (not shown).

In Fig. 6, the first two phase modulation spurs are clearly visible at offset frequencies of 60 kHz and 120 kHz. Similarly, the first sidemode is also visible for each of the systems at

135 kHz. The first sidemode reaches levels of -123 dBc/Hz and -137 dBc/Hz for the DSC50S + RF amplifier and VC-SCOWPD systems, respectively. For the SCOW-OEO operated with RF amplification, the subsequent sidemodes are also present, but gradually decay with offset frequency. The second and third sidemodes, for instance, are at levels of -131 dBc/Hz and -137 dBc/Hz, respectively. Note that the SSA resolution bandwidth is constant from 100 kHz to 780 kHz. In the amplifier-free VC-SCOWPD system, these sidemodes cannot be observed above the noise-floor (~ -150 dBc/Hz). As noted earlier, the low sidemodes are due to the saturation properties of MWP gain in an IMDD link [19]. For certain offset frequencies, the residual harmonics from phase modulation mix with the sidemodes to generate spurs in the phase-noise spectrum. For example, the spur near 535 kHz results from an interaction between the 9th phase modulation harmonic and the 4th sidemode peak. Based on the results of Fig. 4(b) and Fig. 6, we can conclude that RF amplification results in increased sidemode levels during the operation of the OEO. The physics of this process is currently not well understood as it appears that the RF amplifier affects only the sidemodes and not overall phase-noise. Measurements with other high-performance RF amplifiers have yielded the same results. Furthermore, the observed sidemode enhancement is not limited to electrical means, as we have found intracavity optical amplification (not shown) to behave similarly. In all of these cases, the increase in sidemodes appears primarily in the phase-response (and not amplitude) of the OEO system.

4. Summary

We have demonstrated a 3-GHz amplifier-free slab-coupled optical waveguide optoelectronic oscillator (SCOW-OEO) with low phase-noise (< -120 dBc/Hz at 1 kHz offset) and ultralow sidemode levels. These sidemodes are indistinguishable from noise on a spectrum analyzer measurement (> 88 dB down from carrier). This performance was achieved with 1.5 km of optical delay and through the use of high-power low-noise SCOW lasers and photodiodes. We have also evaluated the effect of RF amplification on the phase-noise of the SCOW-OEO. The OEO's operation is significantly degraded by amplifier noise except in the cases when the highest performance amplifiers are used. We found that the sidemode suppression, however, always degrades with amplification, even with the use of low flicker noise amplifiers. Currently, fiber nonlinearities prevent the use of longer delays in the SCOW-OEO system. Once these limitations are circumvented, we expect 20 dB improvement in phase noise through a factor of 10 increase in loop delay (from 1.5 km to 15 km).

Acknowledgments

The authors would like to thank Professor Rajeev J. Ram of the Massachusetts Institute of Technology for valuable discussions.